

# Distinguishing DNA by Analog-to-Digital-like Conversion by Using Optofluidic Lasers\*\*

Yuze Sun and Xudong Fan\*

Distinguishing a target DNA from a counterpart that has a single base mismatch provides critical information for disease diagnosis, personalized medicine, and basic biochemical research.<sup>[1–3]</sup> In traditional, fluorescence-based detection, samples are placed in a cuvette, and a DNA probe is used to hybridize with the target DNA and generate a fluorescent signal. However, because of the small difference in the binding affinity for the DNA probe between the target and the strand with a single base mismatch, the discrimination ratio between the resulting fluorescence is almost unity,<sup>[4–8]</sup> which makes it difficult to directly and selectively detect the target DNA from a pool of mismatched DNA strands.<sup>[9,10]</sup>

Herein, we describe a system for the highly specific intracavity detection of DNA that uses an optofluidic laser. This type of laser is an emerging technology that synergistically integrates a dye laser and microfluidics for miniaturized laser sources, easy sample delivery, and extremely small sample volumes.<sup>[11–13]</sup> In our detection system, DNA samples and probes are incorporated as part of the laser gain medium. Stimulated laser emission, rather than fluorescence (that is, spontaneous emission), is employed as the sensing signal to achieve conversion that is similar to analog-to-digital, which significantly amplifies the small intrinsic thermodynamic difference between the target and its single base mismatched counterpart. A perfectly matched (PM) DNA, a single base mismatched (SM) DNA, and a molecular beacon (MB) probe were used as a model system. A theoretical analysis was performed to elucidate the underlying intracavity detection principle. Then, a discrimination ratio (that is,  $R = I_{PM}/I_{SM}$ , where  $I_{PM}$  and  $I_{SM}$  is the light intensity generated by PM DNA and SM DNA, respectively) of 240:1 was achieved experimentally between PM DNA and SM DNA, which is an increase of over two orders of magnitude relative to the fluorescence-based method. The selective detection of PM DNA from a pool of SM DNA at a concentration ratio of 1:50 is presented. This system can also distinguish more complicated DNA sequences, such as a breast cancer sequence from a corresponding sequence that contains a single point mutation, in both buffer and serum.

An MB is a DNA probe with a stem-loop structure and a dye as well as a quencher attached to each end of the

sequence (Figure 1a).<sup>[10,14–17]</sup> Both PM DNA and SM DNA are able to hybridize with the MB. Consequently, a fraction of MBs open and generate fluorescence. This fluorescence-based detection (see the detailed analysis in Section I A in the

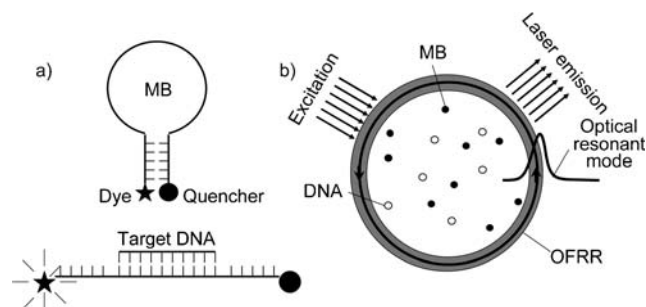


**Figure 1.** a) MB fluorescence is quenched when it is in the closed state. MB fluorescence is restored upon hybridization with the target DNA. b) Intracavity DNA detection and differentiation with the OFRR laser.

Supporting Information) can be regarded as “analog” detection, in which a small thermodynamic difference between PM DNA and SM DNA results in a small difference in the fluorescence signal. Figure S1 in the Supporting Information shows an example of the fluorescence from PM DNA and SM DNA, which has a low discrimination ratio.

In our intracavity DNA detection system, an optofluidic ring resonator (OFRR) is used as the laser cavity. As illustrated in Figure 1b, the OFRR consists of a piece of glass capillary in which the cross-section forms the ring resonator and supports the circulating optical resonant mode with an extremely high Q factor ( $> 10^7$ ).<sup>[18–20]</sup> The evanescent field of the optical mode extends into the core and interacts with the gain medium near the inner surface of the OFRR, thus providing the optical feedback for lasing. When placed in the OFRR, the MB becomes the laser gain medium, which is modulated by the conformational state of the MB through the hybridization with the DNA molecules of interest. Although a small difference in binding affinity between PM DNA and SM DNA causes only a small change in the laser gain coefficient, it is this small change that is amplified into orders of magnitude differences in the emission intensity because of the strong optical feedback that is provided by the OFRR. The detailed analysis of differentiating between PM DNA and SM DNA with the MB-OFRR laser is given in the Supporting Information.

The MB-OFRR laser can be described as a four-energy-level dye system. The corresponding lasing threshold,  $I_{th}$ , can be written as Equation (1),

[\*] Dr. Y. Sun, Prof. Dr. X. Fan  
Biomedical Engineering Department, University of Michigan  
1101 Beal Avenue, Ann Arbor, MI 48109 (USA)  
E-mail: xsfan@umich.edu

[\*\*] We thank the National Science Foundation (ECCS-1045621 and CBET-1037097) for financial support.

Supporting information for this article is available on the WWW under <http://dx.doi.org/10.1002/ange.201107381>.

$$I_{\text{th}} = \gamma / (F - \gamma) \quad (1)$$

where  $\gamma$  is the minimal fraction of the dyes in the excited state that is required for lasing. It is fixed for a given laser cavity, dye, and quencher.  $F$  is the fraction of the MBs in the open state. Equation (1) is central in differentiating between PM DNA and SM DNA. First, it requires that a minimal fraction of MBs must be open (that is,  $F = \gamma$ ) to achieve lasing. Second, it shows that the small difference in  $F$  between PM DNA and SM DNA can be significantly enlarged in the lasing threshold, particularly at low DNA/MB ratios, as shown in Figure S2 in the Supporting Information. Therefore, PM DNA and SM DNA can be differentiated by ramping the pump intensity. Once the pump intensity is above the lasing threshold for PM DNA, but below that for SM DNA, extremely strong laser emission is detected for PM DNA whereas only negligible fluorescence background is detected for SM DNA. Theoretically, a discrimination ratio as high as  $10^5:1$  can be achieved.<sup>[21]</sup> Such deep fluorescence background suppression mimics the analog-to-digital conversion in electronics, which eliminates the contribution from SM DNA (regardless of the SM DNA concentration over a large range, see below) and generates high signal fidelity to detect the presence of PM DNA. It should be emphasized that although we use MB as the model system, this detection system is applicable to any other fluorescent reporters, such as DNA-binding dyes<sup>[22]</sup> (as long as they report the difference between PM DNA and SM DNA) and other microlasers<sup>[11–13]</sup> (as long as they are compatible with liquid-phase detection).

To experimentally differentiate between PM DNA and SM DNA with the OFRR laser, the simple DNA sequences polyadenosine and polyadenosine with a single point mutation were used.<sup>[10]</sup> The corresponding MB was labeled with 6-carboxyfluorescein (FAM) and 4-((4-(dimethylamino)phenyl)azo)benzoic acid (DABCYL). The details of the samples and their characterization are given in Table S1 and Figure S3 in the Supporting Information. The OFRR laser setup is illustrated in Figure S4 in the Supporting Information. Figure 2 shows the comparison of MB emissions in the presence of PM DNA or SM DNA under the same experimental conditions. In the presence of PM DNA, multiple strong lasing peaks were detected at longer wavelengths in the FAM emission spectrum, which is typical for a multimode dye laser, such as the OFRR.<sup>[20,23]</sup> In sharp contrast, only weak, featureless fluorescence was observed in the presence of SM DNA. If the spectrally integrated emission intensity is used as the sensing signal, a discrimination ratio of 240:1 is obtained between PM DNA and SM DNA, which is an improvement of more than two orders of magnitude over conventional, fluorescence-based DNA detection that uses the same MB (see Figure S3 in the Supporting Information).

As discussed above, the difference between PM DNA and SM DNA is intrinsically reflected in their respective lasing thresholds. Figure 3a shows the output intensities that were extracted from the MB emission spectra as a function of the pump energy density. For PM DNA, a lasing threshold of approximately  $1 \mu\text{J mm}^{-2}$  was achieved (Figure 3a, inset). In contrast, no lasing emission was detected for SM DNA, even with the highest possible energy density from the pump laser

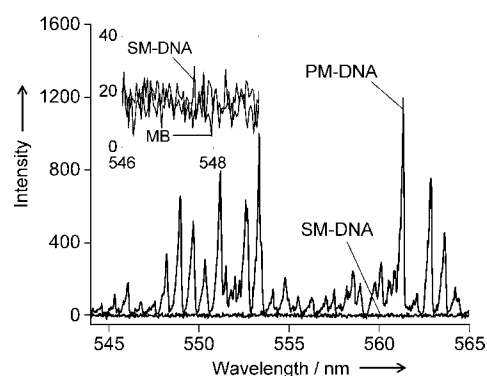


**Figure 2.** Comparison of the MB emission spectrum in the presence of PM DNA or SM DNA. The DNA/MB molar ratio is 1:1. MB concentration was fixed at  $50 \mu\text{M}$ . The pump energy density was  $25.6 \mu\text{J mm}^{-2}$  at  $490.7 \text{ nm}$ . The background fluorescence from MB alone is subtracted. Inset: part of the fluorescence spectra for the MB alone and in the presence of SM DNA.

( $100 \mu\text{J mm}^{-2}$ ). Such a huge difference in the lasing threshold is a result of the inability of SM DNA to open adequate MBs to satisfy the requirement of  $F > \gamma$  in Equation (1). After increasing the concentrations of DNA and keeping the concentration of MB unchanged, lasing can be achieved for both PM DNA and SM DNA, as shown in Figure 3b–d, with a progressively decreasing lasing threshold. The inset in Figure 3b is a plot of the normalized thresholds that were obtained from the experiments and calculated from Equations S12–S14 in the Supporting Information. The qualitative agreement between these two results suggests that our model reflects the essence of the OFRR laser system and provides an insight into the corresponding DNA differentiation system.

Based on Equations S15 and S16 in the Supporting Information, the output power is linearly proportional to the pump energy density above the lasing threshold or to the fraction of MBs that are open ( $F$ ) above the minimal fraction of MBs that is required for lasing ( $\gamma$ ). Figure 4 is a plot of the lasing emission spectra for different concentrations of PM DNA with a fixed concentration of MB at a fixed pump energy density. The experimental results agree well with the theoretical predictions. This agreement not only validates our model further, but also suggests that the lasing emission intensity can be used to quantify the concentration of PM DNA.

Direct and specific detection of PM DNA from a pool of SM DNA provides an excellent test to examine the selectivity of DNA detection. The regular fluorescence signal from a DNA mixture contains a comparable contribution from both PM DNA and SM DNA and, thus, becomes very difficult to resolve. In many conventional MB-based DNA detection systems, pure PM DNA and pure SM DNA are first detected individually, then the fraction of detectable PM DNA is deduced.<sup>[4,5,9,10]</sup> In contrast, as the intracavity detection provides the “clear-cut” analog-to-digital-like conversion, the signal that is generated by the presence of SM DNA is completely suppressed (over a large concentration range) and thus does not interfere with the positive identification of PM DNA. To verify this, the pump intensity was set to slightly

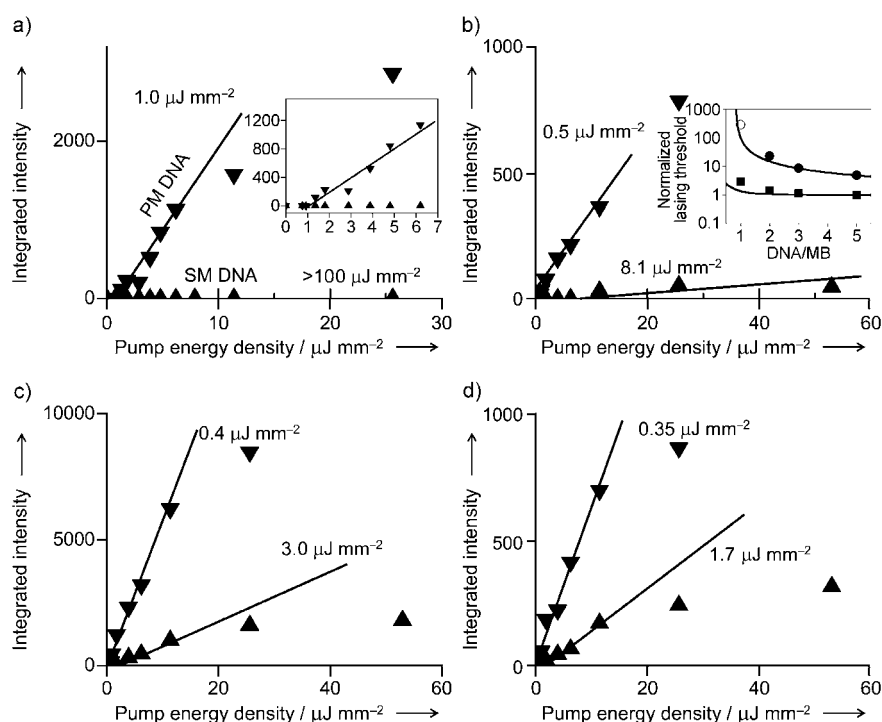


**Figure 3.** Spectrally integrated MB emission intensity versus the pump energy density for various concentrations of PM DNA and SM DNA.  $[DNA]/[MB] = 1:1, 2:1, 3:1$ , and  $5:1$  for panels a), b), c), and d), respectively. Upper and lower data points in each Figure are for PM DNA and SM DNA, respectively. Solid lines are the linear fit for the pump energy density above the lasing threshold. The lasing threshold is labeled near the corresponding linear fit lines. The MB concentration was fixed at  $50 \mu\text{M}$ . Spectra were integrated from  $544 \text{ nm}$  to  $565 \text{ nm}$ . Inset in (a): Magnification of (a). Inset in (b): Normalized lasing thresholds for the various concentrations of PM DNA and SM DNA that are presented in (a), (b), (c), and (d). SM DNA =  $\bullet$  and PM DNA =  $\blacksquare$ . The open circle at DNA/MB ratio =  $1:1$  was obtained by using the estimated threshold ( $100 \mu\text{J mm}^{-2}$ ), as no lasing was achieved. Solid lines are the magnified part of Figure S2. Both experimental and theoretical results are normalized to the threshold that corresponds to  $[PM \text{ DNA}]/[MB] = 5:1$ .

higher than the threshold for PM DNA at a  $2:1$  molar ratio with respect to the MB, but lower than that for SM DNA (see Figure S2 in the Supporting Information for an illustration). As a negative control, no lasing emission was detected for SM DNA (spectrally integrated intensity: approximately 10) even at an extremely high concentration ( $[SM \text{ DNA}]/[MB] = 100:1$ , Figure 5a–e). However, strong lasing emission was detected (spectrally integrated intensity: approximately 300) when small amount of PM DNA was added, thus 1 PM DNA molecule was directly and positively identified in the presence of 50 SM DNA molecules in the mixture.

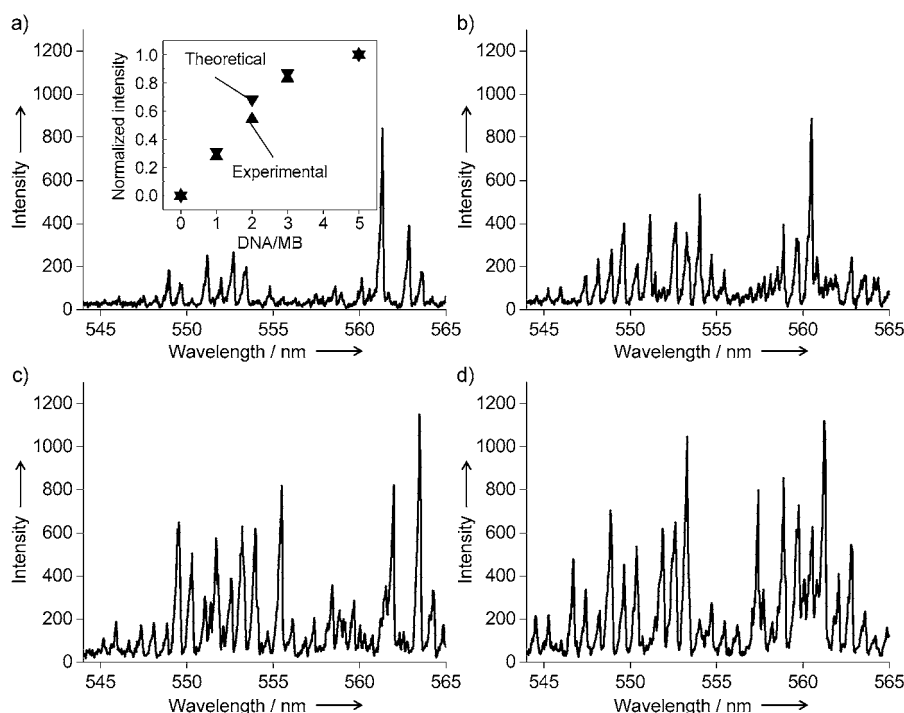
To further validate our method, a more complicated DNA sequence from the breast cancer and ovarian cancer gene BRCA1, as well as a corresponding sequence that contained a single point mutation were tested. The sequences for the MB, PM DNA, and SM DNA are given in Table S2 in the Supporting Information. For the SM DNA sequences, the mutation was either in the middle (SM-M) or at the end (SM-E) of the sequence. For comparison, all the sequences are the same as those in Ref. [7], in which the conventional MB method was used and showed a very small discrimination ratio of  $1.5:1$  ( $1.2:1$ ) between PM DNA and SM-M (SM-E)

DNA. Figure S5a in the Supporting Information shows the spectra for  $[DNA]/[MB] = 1:1$  and clearly demonstrates that our method is capable of differentiating PM DNA and SM DNA (discrimination ratio greater than 100), regardless of the position of the mismatch. With an increased concentration of DNA (Figure S5b in the Supporting Information), lasing emission can also be achieved for SM-E DNA, but not for SM-M DNA. Such a difference between SM-E DNA and SM-M DNA is a result of the higher affinity of SM-E DNA for the MB. This result is consistent with the conventional MB method.<sup>[7]</sup> Note that although both PM DNA and SM-E DNA can lase at high concentrations, the difference in the corresponding lasing threshold still allows differentiation between PM DNA and SM DNA (SM-E and SM-M). As shown in Figure S6 in the Supporting Information, for a given DNA concentration, PM DNA has the lowest lasing threshold, whereas SM-M DNA has the highest.

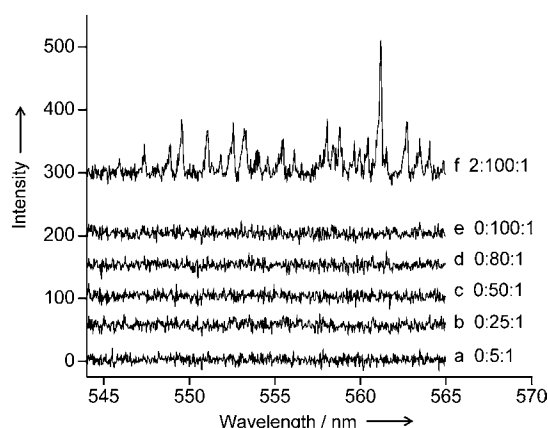
All the experiments discussed above were performed in buffer solution. When samples are in other media, such as serum, the value of  $I$  or  $\gamma$  may change. For example, when serum is used,  $\gamma$  may increase because of the additional loss in the OFRR that is introduced by serum absorption. Nevertheless, the detection principle should still be valid. As shown by curve 4 in

Figure S5b in the Supporting Information, the lasing emission can be detected even when the DNA samples were in 50% serum. The corresponding lasing threshold curve that is plotted in Figure S6d in the Supporting Information shows that the lasing threshold is approximately  $2.5 \mu\text{J mm}^{-2}$ , which, as expected, is much higher than when the sample is in buffer solution. By using Equation S13 in the Supporting Information and assuming that serum does not affect the affinity between DNA and the MB (that is,  $I_{\text{serum}} = I_{\text{buffer}}$ , where  $I_{\text{serum(buffer)}}$  is the fraction of the open MBs when samples are in serum (buffer)), we estimate that  $\gamma_{\text{serum}} = 2.76\gamma_{\text{buffer}}$ . Because of this increased  $\gamma$ , the necessary condition,  $I_{\text{serum}} > \gamma_{\text{serum}}$ , could no longer be satisfied for SM-E DNA and SM-M DNA in serum for either  $[DNA]/[MB] = 1:1$  or  $5:1$ . Consequently, no lasing emission was detected for SM-E DNA or SM-M DNA in serum, thus allowing the differentiation of PM DNA from SM DNA.

In conclusion, by using PM DNA, SM DNA, and MB as a model system, we theoretically analyzed and experimentally demonstrated an optofluidic laser intracavity detection system that is capable of distinguishing two DNA sequences that have small thermodynamic differences, and can even



**Figure 4.** Lasing emission spectrum of the MB hybridized with various concentrations of PM DNA. [PM DNA]/[MB] = 1:1, 2:1, 3:1, and 5:1 for panels a), b), c), and d), respectively. The MB concentration was fixed at  $50 \mu\text{M}$  and the pump energy density was  $6.2 \mu\text{J mm}^{-2}$  at  $490.7 \text{ nm}$ . Inset in (a): Spectrally integrated intensity from  $544 \text{ nm}$  to  $565 \text{ nm}$  (normalized to the highest output) that were obtained from (a)–(d), along with the normalized theoretical results based on Equation S16 in the Supporting Information.



**Figure 5.** Selective detection of PM DNA from high concentrations of SM DNA. a)–e) Negative controls. [PM DNA]/[SM DNA]/[MB] is labeled on the right side of the corresponding graphs. f) Positive control. The MB concentration was fixed at  $50 \mu\text{M}$  and the pump energy density was  $0.8 \mu\text{J mm}^{-2}$ . Curves are vertically shifted for clarity.

directly detect PM DNA from mixed samples with unprecedented selectivity. The same system can readily be adapted for linear DNA probes,<sup>[24]</sup> other fluorescent reporters, such as DNA-binding dyes,<sup>[22,24]</sup> and other types of optofluidic lasers,<sup>[11–13]</sup> as well as other DNA sequences with small thermodynamic differences, such as methylated DNA.<sup>[8]</sup> Future work will include differentiation of methylated

DNA,<sup>[8]</sup> detection of microRNA,<sup>[25]</sup> high-resolution DNA melting analysis,<sup>[8,22]</sup> and even monitoring of the biological processes that occur inside a cell.<sup>[26]</sup>

Received: October 19, 2011

Revised: November 29, 2011

Published online: December 23, 2011

**Keywords:** DNA · lasers · molecular beacons · optofluidics · sensors

- [1] T. K. Christopoulos, *Anal. Chem.* **1999**, *71*, 425–438.
- [2] L. J. van't Veer, R. Bernards, *Nature* **2008**, *452*, 564–570.
- [3] P. A. Jones, S. B. Baylin, *Nat. Rev. Genet.* **2002**, *3*, 415–428.
- [4] X. Liu, W. Farmerie, S. Schuster, W. Tan, *Anal. Biochem.* **2000**, *283*, 56–63.
- [5] S. Song, Z. Liang, J. Zhang, L. Wang, G. Li, C. Fan, *Angew. Chem.* **2009**, *121*, 8826–8830; *Angew. Chem. Int. Ed.* **2009**, *48*, 8670–8674.
- [6] K. Lee, L. K. Povlich, J. Kim, *Adv. Funct. Mater.* **2007**, *17*, 2580–2587.
- [7] A. Hsieh, P. Pan, A. Lee, *Microfluid. Nanofluid.* **2009**, *6*, 391–401.
- [8] C. M. Rodríguez López, B. G. Asenjo, A. J. Lloyd, M. J. Wilkinson, *Anal. Chem.* **2011**, *82*, 9100–9108.
- [9] G. Bonnet, A. Libchaber, *Physica A* **1999**, *263*, 68–77.
- [10] B. Dubertret, M. Calame, A. J. Libchaber, *Nat. Biotechnol.* **2001**, *19*, 365–370.
- [11] Z. Li, D. Psaltis, *Microfluid. Nanofluid.* **2007**, *4*, 145–158.
- [12] A. R. Hawkins, H. Schmidt, *Handbook of Optofluidics*, CRC, Boca Raton, **2010**.
- [13] X. Fan, I. M. White, *Nat. Photonics* **2011**, *5*, 591–597.
- [14] S. Tyagi, F. R. Kramer, *Nat. Biotechnol.* **1996**, *14*, 303–308.
- [15] G. Bonnet, S. Tyagi, A. Libchaber, F. R. Kramer, *Proc. Natl. Acad. Sci. USA* **1999**, *96*, 6171–6176.
- [16] A. Tsourkas, M. A. Behlke, Y. Xu, G. Bao, *Anal. Chem.* **2003**, *75*, 3697–3703.
- [17] W. Tan, K. Wang, T. J. Drake, *Curr. Opin. Chem. Biol.* **2004**, *8*, 547–553.
- [18] S. I. Shopova, H. Zhu, X. Fan, P. Zhang, *Appl. Phys. Lett.* **2007**, *90*, 221101.
- [19] S. Lacey, I. M. White, Y. Sun, S. I. Shopova, J. M. Cupps, P. Zhang, X. Fan, *Opt. Express* **2007**, *15*, 15523–15530.
- [20] Y. Sun, S. I. Shopova, C.-S. Wu, S. Arnold, X. Fan, *Proc. Natl. Acad. Sci. USA* **2010**, *107*, 16039–16042.
- [21] A. E. Siegman, *Lasers*, University Science Books, Sausalito, CA, **1986**.
- [22] G. H. Reed, C. T. Wittwer, *Clin. Chem.* **2004**, *50*, 1748–1754.
- [23] H.-J. Moon, Y.-T. Chough, K. An, *Phys. Rev. Lett.* **2000**, *85*, 3161–3164.
- [24] W. Lee, X. Fan, unpublished results.
- [25] W. J. Rhee, P. J. Santangelo, H. Jo, G. Bao, *Nucleic Acids Res.* **2008**, *36*, e30.
- [26] M. C. Gather, S. H. Yun, *Nat. Photonics* **2011**, *5*, 406–410.